Vision Res. Vol. 25, No. 9, pp. 1305–1315, 1985
Printed in Great Britain.

0042-6989/85 $3.00 + 0.00

THE STILES–CRAWFORD EFFECT IN THE EYE OF THE BLOWFLY, *CALLIPHORA ERYTHROCEPHALA*

J. H. VAN HATEREN
Department of Biophysics, Laboratory for General Physics, University of Groningen, Groningen, The Netherlands

(*Received* 8 *June* 1984; *in revised form* 22 *November* 1984)

Abstract—Stiles–Crawford-like effects (that is, directional sensitivity of the retina) were investigated in the fly's eye. Intracellular recordings from the visual sense cells were made, and the radiation patterns emerging from the photoreceptors with antidromic light were photographed, and evaluated with a microdensitometer. The measurements from both methods agree well, and can be satisfactorily described by a theoretical model based on waveguide theory. Clear radiation patterns from the first and second order modes were observed at the level of the cornea. As in the vertebrate eye, the photoreceptors are aligned towards the center of the lens, a phenomenon for which a theoretical explanation is proposed.

Stiles–Crawford effect Blowfly, *Calliphora erythrocephala* Photoreceptor optics

INTRODUCTION

The Stiles–Crawford effect (Stiles and Crawford 1933; Stiles, 1937) is the phenomenon that the perceived brightness of light penetrating the pupil of an eye depends on the place of entrance in the pupil. Light entering centrally is more effective than light entering peripherally. In man it can be measured psychophysically by focusing a light beam at different positions in the pupil, and comparing its brightness with a second beam at a constant position (reviews: Crawford, 1972; Enoch and Bedell, 1981). The effect is considered to be primarily retinal, probably originating in the photoreceptors (for photopic vision the cones).

The explanation of the effect is not yet completely established. Basically, there are two competing explanations. The first one states that the effect is caused by the acceptance profile of the photoreceptors for light rays coming from different directions (O'Brien, 1946; Enoch, 1963). Because photoreceptors function as dielectric waveguides (Toraldo di Francia, 1949; Enoch, 1963), a full explanation must consider waveguide effects (e.g. Snyder and Pask, 1973; De Groot, 1980). The second explanation of the Stiles–Crawford effect states that the photoreceptors deviate from perfect alignment towards the center of the lens in a random (Gaussian) way (Safir and Hyams 1969). Light entering the pupil at different positions then excites different numbers of the many photoreceptors contributing to the psychophysically measured effect.

A way to distinguish these two possibilities experimentally, is to measure the response of single visual sense cells. This is difficult to do psychophysically, and electrophysiological data on the acceptance profiles of photoreceptors are relatively scarce (but see e.g. Baylor and Fettiplace 1975). Therefore, a study of these profiles was undertaken in the eye of the blowfly. Despite the many differences between the vertebrate lens-eye and the fly compound eye, the basic optical configuration is remarkably similar in both eye-types, as will be explained below. In fly, electrophysiological recordings from single photoreceptors can be made on an intact animal (with an intact dioptrical apparatus); moreover, quantitative optical measurements can be made on the radiation coming from the photoreceptors when the normal light direction is reversed (antidromic illumination, cf. Enoch 1963); finally, the detailed knowledge of the dioptrical system (e.g. Kirschfeld and Franceschini, 1968; Franceschini, 1975; Stavenga, 1975; Beersma, 1979; van Hateren, 1984; review: Hardie, 1985) allows the calculation of the effect as well, with a theory based on wave-optics. Thus, an integrated electrophysiological, optical, and theoretical approach to the problem will be presented in this paper.

The basic element of the fly compound eye, the ommatidium, is shown in Fig. 1. The compound eye consists of many of these ommatidia, each pointing to a different direction in space. Each ommatidium of the fly includes a lens and seven waveguides (rhabdomeres), the tips of which lie in the focal plane of the lens. These rhabdomeres, each belonging to a visual sense cell, are filled with visual pigment, and can be considered as analogues of the vertebrate cones and rods. They are numbered as shown in the figure. The visual sense cells react with graded depolarizing potentials upon illumination. Fly rhabdomeres function as lightguides by the phenomenon of internal total reflection, because their refractive index is somewhat higher than the refractive index of the surrounding media. Actually, the light propagation through these rhabdomeres must be described with wave-optics, because of their small diameter. It

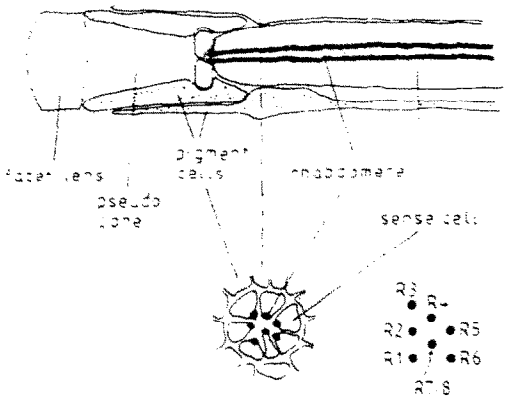

Fig. 1. An ommatidium of the fly's eye. Light is imaged by the corneal lens through the optically homogeneous pseudocone onto the tips of the rhabdomeres, specializations of the sense cell membrane that contain the visual pigment and function as lightguides. The rhabdomeres are numbered as indicated.

turns out, that light can only propagate in stable light patterns, the so-called modes. The shape and number of the modes is determined by the V-number of the waveguide, with

$$V = \frac{2\pi b}{\lambda}(n_1^2 - n_2^2)^{1/2} \qquad (1)$$

where b is the radius of the waveguide, λ the free space wavelength of the light, n_1 the refractive index inside the waveguide, and n_2 the refractive index outside the fiber. For $V \leqslant 2.4$ only the circularly symmetrical first order mode (01) can propagate, for $2.4 < V \leqslant 3.8$ also the bilobed second order mode (11), and for $V > 3.8$ higher order modes as well. For further details on waveguide theory see Marcuse (1974), Snyder (1975), Horowitz (1981), and Snyder and Love (1983).

METHODS

Animals

All experiments were performed on females of the blowfly *Calliphora erythrocephala* (wild type). All flies had a high content of xanthopsin (the fly visual pigment, Vogt 1983), and were taken from a culture originating from specimens caught in the wild. Electrophysiological measurements were made on ten flies, optical measurements on twelve flies. For seven flies theoretical calculations were made as well. The experimental results and theoretical interpretations were similar for all flies.

Preparation

Unanaesthetised animals were fixed with wax, and mounted on an x-y-z stage. Care was taken not to impair ventilation. A small hole was cut in the back of the fly's head, through which a small plastic lightguide was inserted for giving antidromic light. Moreover, a small hole was cut in the dorsal part of the cornea (Hardie, 1979; Smakman *et al.*, 1984). The hole was covered with silicon grease to prevent desiccation. Through this hole a glass micro-electrode was inserted in the retina. The optics of the eye was thoroughly checked before and after the experiment by inspection of the deep pseudopupil, the farfield radiation pattern, and the cornea. Usually no optical deterioration was observed, if the hole in the cornea was made with much care.

Optical set-up

The optical instrument (Fig. 2) is an extension of the one described previously (van Hateren 1984). The instrument can be used both for observing the radiation coming from the eye with antidromic illumination, and for stimulating the eye with orthodromic illumination. The stimulus is imaged in the planes H_1 and H_2. In plane H_1 an image of the farfield radiation pattern of the eye is cast (when using lens L_4), or an image of the cornea (when using lens L_3). With L_4 it is possible to measure angular sensitivities of the entire lens-photoreceptor system, whereas with L_3 the Stiles–Crawford effect can be measured. Both stimulus and cornea (or farfield) can be seen at the same time by means of a pellicle half-mirror (P). The stimulus is seen in the plane H_2 (where a mirror is placed), and the cornea in the plane H_1.

To check that these two images, which are seen simultaneously by the observer, correspond to the real situation as seen by the fly (and that they are not displaced relative to each other), a frosted glass was inserted in the plane H_1. It turned out that the image of the stimulus seen in plane H_2 did indeed coincide with the image on the frosted glass in the plane H_1.

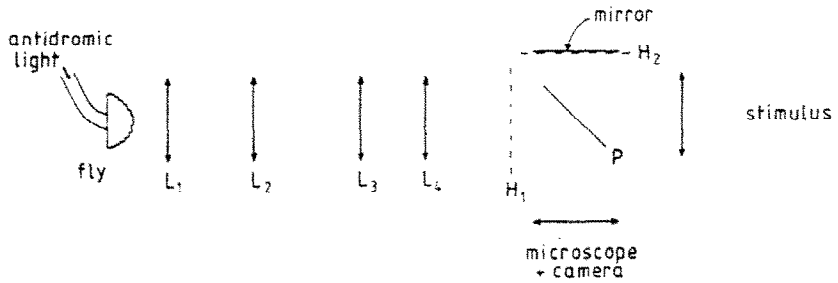

Fig. 2. The optical set-up. The cornea of the fly can be seen simultaneously with the stimulus by the pellicle half-mirror P. L_1: Leitz, Pl fl 10/0.30; L_2: doublet $f = 80$ mm; L_3: doublet, $f = 20$ mm; L_4: Photar, $f = 50$ mm.

Actually, this is a consequence of the design of the instrument, because the image of the stimulus seen by the observer is coplanar with the mirror in the plane H_2, which implies that the exact angular position of this mirror is not very critical for the position where the stimulus is seen. Moreover, the exact angular position of the pellicle is not very critical either, because the images of both cornea and stimulus are displaced in the same direction by angular displacements of the pellicle, as can be shown by applying some geometrical optics. Further details on the optical set-up can be found in the legend of Fig. 2 and in van Hateren (1984).

Electrophysiological measurements

Light of a Xenon arc lamp was chopped, and filtered by a heat filter, neutral density filters, a motor-driven neutral density wedge (Smakman and Pijpker 1983), and a Balzers K-filter (half-width approximately 50 nm). This light was imaged on one end of a flexible lightguide, the other end of which served as the stimulus for the electrophysiological measurements. This end, mounted on a perimeter that could be swept through the visual field, was imaged on the cornea as a light spot with a diameter of approximately 2 μm (and approximately 20° in the farfield).

The intracellular recordings from visual sense cells (R1-6) were made with a conventional set-up for intracellular electrophysiology (Muijser, 1979; Smakman, *et al.*, 1984). The 3M KAc-filled electrodes had resistances of 150–200 MΩ in Ringer's solution. The response of the visual sense cells was clamped at a certain level (6 mV) by feedback through the motor-driven neutral density wedge (Smakman and Pijpker, 1983; Smakman *et al.*, 1984). By this constant criterion method the adaptation of the cell was maintained at a constant level. The position of the neutral density wedge was a direct measure of the sensitivity of the cell for the various positions of the stimulus on the corneal lens. The sensitivity is defined as the reciprocal of the light intensity necessary to reach the criterion response.

Optical measurements

Light of a second Xenon arc lamp was filtered by a heat filter and a Balzers K-filter. It was focused on a small lightguide, the other end of which was inserted in the fly's head. This light propagated backwards through the rhabdomeres, and illuminated the corneal lenses from behind. The resulting radiation patterns are not equally bright for all wavelengths (see Fig. 5), because the light travels through (and is filtered by) nervous tissue and the basal membrane. Moreover, the light is partially absorbed by the visual pigment in the rhabdomeres. The fly visual pigment absorbs maximally at a wavelength of 490 nm; therefore, optical measurements were not possible for 500 nm, and only with long exposure times for 450 nm. The cornea was photographed on Tri-X (5 min for filters K60 and K55, 50 min for K45). The film was developed and calibrated as previously described (van Hateren, 1984), and subsequently scanned with a microdensitometer (Joyce, Loeble & Co., MK3C). The densities thus obtained were transformed to intensities of the light at the corneal level. Both sides of the curves were averaged because the curves were approximately symmetrical.

THEORY

For electrophysiological measurements the photoreceptors are stimulated by focusing a light beam at the level of the cornea. Both the focused light spot on the cornea and the receptor entrance are small ($\simeq 2\,\mu$m) compared to the distance between them ($\simeq 100\,\mu$m). Thus the photoreceptors are in effect illuminated by a plane wave. The theory used for calculating the excitation of modes in a waveguide by plane wave illumination is summarized in the Appendix.

For optical measurements of the Stiles–Crawford effect the direction of the light is reversed (antidromic light), and the radiation patterns emerging from the photoreceptors are observed. It can be shown theoretically (by an argument similar to the one presented in van Hateren, 1984) that if a photoreceptor can propagate only the first order mode, the shape of the farfield radiation pattern of the receptor is identical to that of its sensitivity profile when stimulated by a plane wave coming from various directions. Thus, for a single mode photoreceptor the optical measurements must yield the same results as electrophysiological measurements of the Stiles–Crawford effect. This is generally not true, however, when higher order modes can also propagate [for the shorter wavelengths, see equation (1)]. The reason is that the relative weighting of the modes (the fraction of the total guided power each carries) is generally different for the optical and electrophysiological methods. First, the electromagnetic field exciting the modes is different for orthodromic and antidromic light, as the orthodromic light is neatly focussed on the receptors by the facet lenses, whereas the antidromic light has travelled through the underlying nervous tissue. Second, the light transmitted through the photoreceptors is measured for the optical experiments, while the light absorbed in the photoreceptors is measured for the electrophysiological experiments. So because the various modes are absorbed independently of each other and with different efficiencies, the resulting relative weighting of the modes is entirely different for the two methods.

The case of only one mode is encountered at the longer wavelengths, that is, with V smaller than 2.4. The situation is even then not unambiguous in the fly, however, because more than one sense cell contributes to the radiation towards the lens of one ommatidium. Nevertheless, it will be shown below

that the photoreceptors in an ommatidium are aligned towards the center of the lens. Thus, measurements made at the level of the cornea will give the same result irrespective of the number of sense cells contributing to the radiation. Another complication is the central rhabdomere R7, having a smaller diameter (1 μm) than R1–6 (1.8 μm). It is outnumbered, however, by R1–6, and for the longer wavelengths its radiation pattern is similar to that of R1–6. For shorter wavelengths the central rhabdomere absorbs light efficiently, which makes its contribution to the total radiation pattern negligible.

RESULTS

Alignment

In Fig. 3 it is shown that fly rhabdomeres are aligned towards the center of the lens (as was first noticed by Stavenga, personal communication). The ommatidial lenses were optically neutralized by waterimmersion (Franceschini, 1975), and the radiation from the rhabdomeres photographed at various distances from the lens surface.

The photographs were evaluated with a microdensitometer, allowing precise measurements of the distance between the light beams radiating from rhabdomeres R1 and R3. As we see in Fig. 3, these beams converge towards the lens. This is also the case for other rhabdomere pairs, thus all rhabdomeres converge to a common point. The position of the convergence point in Fig. 3 is at 14 ± 8 μm from the lens surface. Thus one could argue that at the corneal level (where the photographs were made) the superposition of the various radiation patterns might not be perfect. Nevertheless, the maximum error in the alignment ($\simeq 1$ μm at the cornea) is negligible compared to the width of the radiation patterns (half-width $\simeq 15$ μm at the cornea).

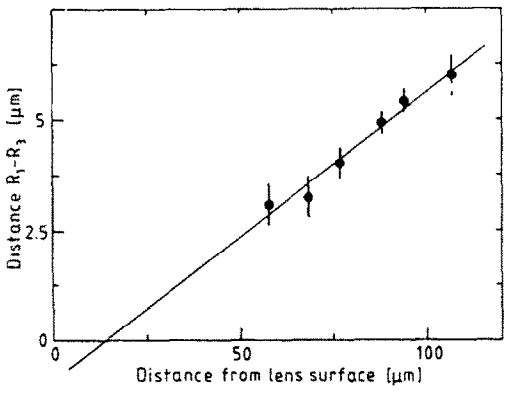

Fig. 3. The alignment of fly rhabdomeres towards the center of the lens. The distance between the centers of the beams radiating from the rhabdomeres R_1 and R_3 is given as a function of the distance from the lens surface, as observed with a waterimmersion objective. Both distances can deviate from the real distances by a constant factor, because the waterimmersion might not completely neutralize the lens.

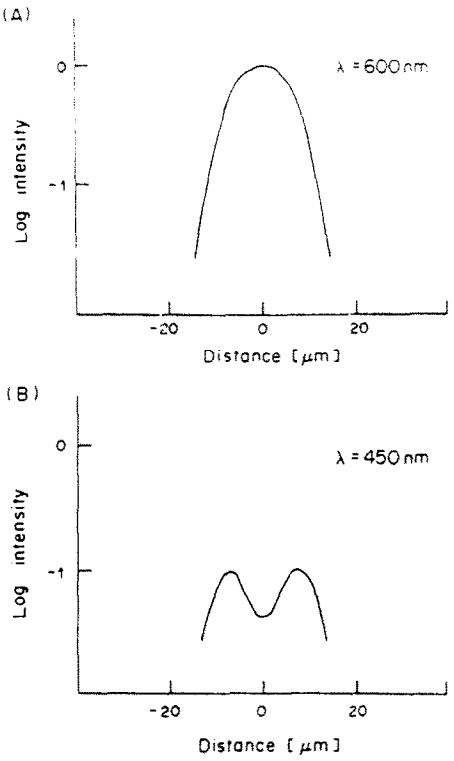

Fig. 5. Densitograms of the photographs shown in Fig. 4. The image of a single lens was scanned on the negative by means of a microdensitometer. Wavelengths: (A) 600 nm; (B) 450 nm.

Observations of modal patterns

Photographs of the cornea of the fly with antidromic illumination are shown in Fig. 4. In Fig. 4(a) the wavelength is 600 nm, and all the lenses are illuminated in a similar way: brightest in the center, and darkening towards their boundary. This can be seen also in the densitogram of one of these lenses in Fig. 5(a). The illumination is approximately circularly symmetrical. For shorter wavelengths the cornea appears dramatically different, as is shown for 450 nm in Fig. 4(b): now the center is darkest, and a bright ring is visible. Again the pattern is approximately circularly symmetrical; a densitogram is shown in Fig. 5(b). The ring-shaped illumination indicates the presence of the second order mode. The radiation from a single second order mode has two lobes (see e.g. Snyder, 1975), but superposition of radiation from second order modes with different angular dependences can yield a circular pattern. Moreover, Fig. 4(b) is a superposition of the radiation from several rhabdomeres, favouring a circularly symmetrical result.

Second order modes can also be observed in the farfield radiation pattern of the entire lens–photoreceptor system (van Hateren, 1984). In that case we are actually looking at the modes at the rhabdomere tips (via the corneal lens). In Fig. 4 we are looking at the (farfield) radiation coming from these modes. Thus, despite the similarity, we should

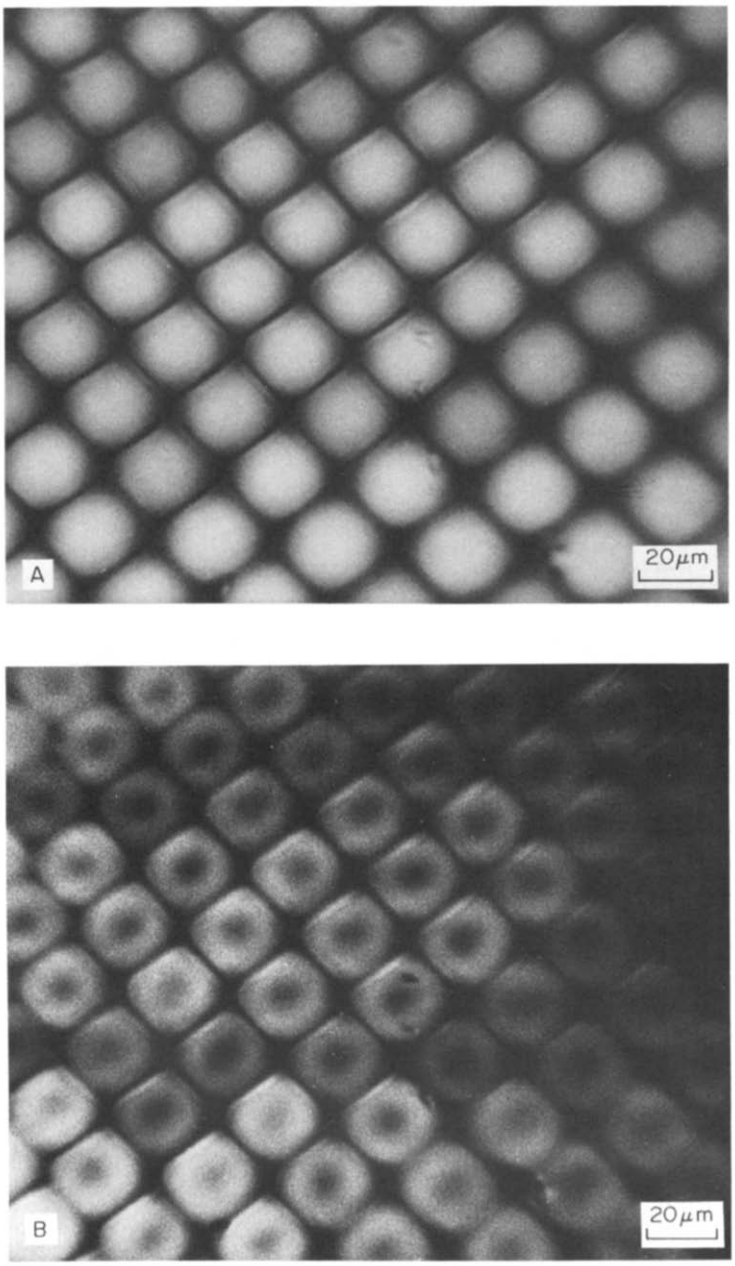

Fig. 4. Photographs of the ventral cornea of the fly, with approximately square lenses. Wavelengths: (A) 600 nm; (B) 450 nm. In (B) radiation from second order modes is seen.

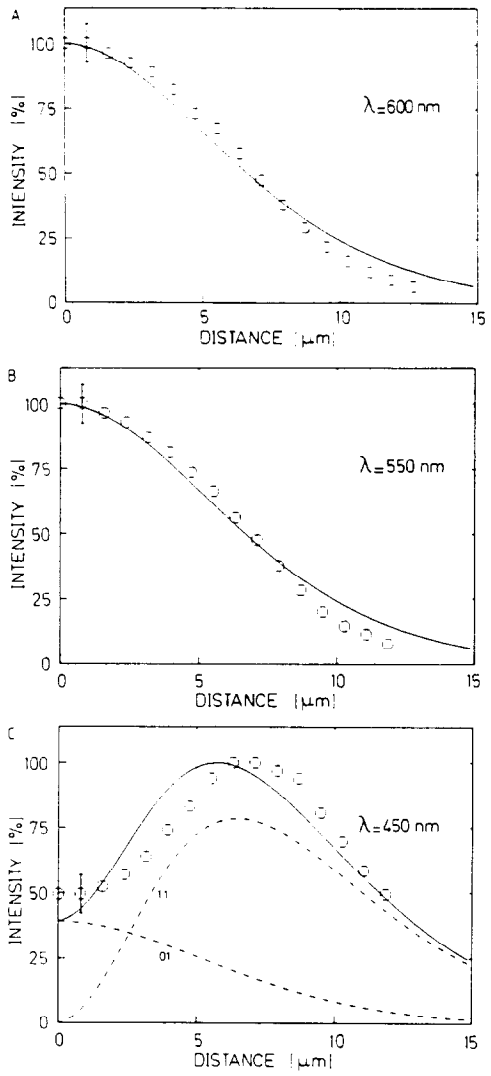

Fig. 6. The intensity of the radiation patterns of the rhabdomeres of one ommatidium (the same as in Fig. 5) as a function of the distance from the center of the facet lens (open circles), and theoretical fits (continuous curves). Focal distance (in air): 70 μm; $\tilde{n} = 0.25$; fiber diameter: 1.8 μm; wavelengths: (A) 600 nm; (B) 550 nm; (C) 450 nm. The lens diameter was 25–30 μm. In (A) and (B) only the first order mode (01) propagates, in (C) also the second order mode (11).

not confuse the mode patterns themselves with their radiation patterns (as in Fig. 4). In fact, the amplitudes of the two are related by Fourier transforms, similar as the diffraction pattern of an aperture is the Fourier transform of the aperture (Goodman, 1968). Modes just happen to be very similar in shape to their Fourier transforms, that is, their far field radiation patterns.

Measurements and theoretical calculations

In Fig. 6 optical measurements with linearized intensity axes are shown, together with theoretical calculations. The theoretical curves were calculated according to the theory summarized in the Appendix. The parameters for the calculations are the wavelength, the fiber diameter, the refractive indices inside and outside the waveguide, and the focal distance. The wavelength is under experimental control; for the fiber diameter a value of 1.8 μm was chosen (Horridge *et al.*, 1976), and for $\tilde{n} = (n_1^2 - n_2^2)^{1/2} = 0.25$ (Beersma *et al.*, 1982). The remaining parameter, the focal distance, is not constant over the eye, and was treated as a free variable, chosen to obtain a reasonable fit (by eye) to the experimental curves. The focal distance is not a completely free variable, however, because it depends on the lens diameter. The F-number of the facet lenses (that is, focal distance divided by lens diameter) has been estimated for *Musca* (Stavenga, 1975), but it is not completely constant over the eye (see Discussion). Nevertheless, the F-number found here by fitting to the experimental data is in reasonable agreement with previously determined F-numbers obtained by different methods (Stavenga, 1975).

In Fig. 6(c) the wavelength was sufficiently short to permit the existence of the second order mode. The relative weighting of the various propagated modes is difficult to calculate, especially for antidromic illumination (for a discussion see the section on Theory and van Hateren, 1984), and the weighting factor was therefore also treated as a free variable. The theoretical calculation in Fig. 6(c) yields a result that is somewhat narrower than the measurements. The reason for this is not clear, but taking into account

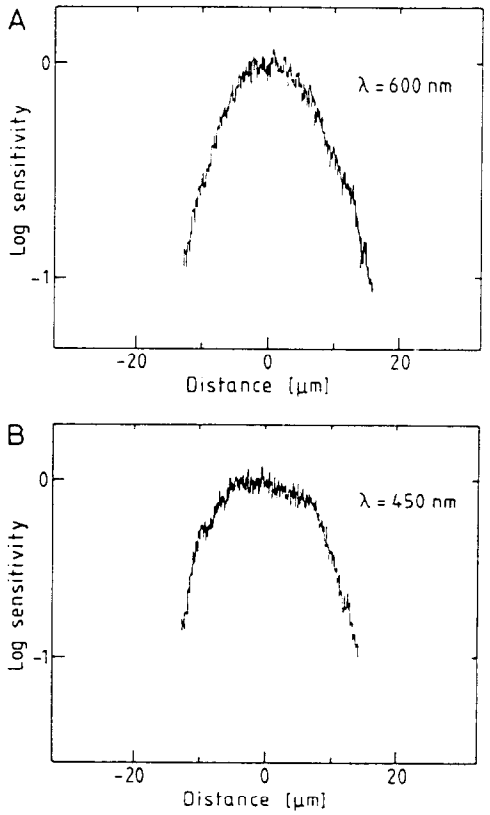

Fig. 7. Electrophysiological measurements of the Stiles–Crawford effect. Wavelengths: (A) 600 nm; (B) 450 nm.

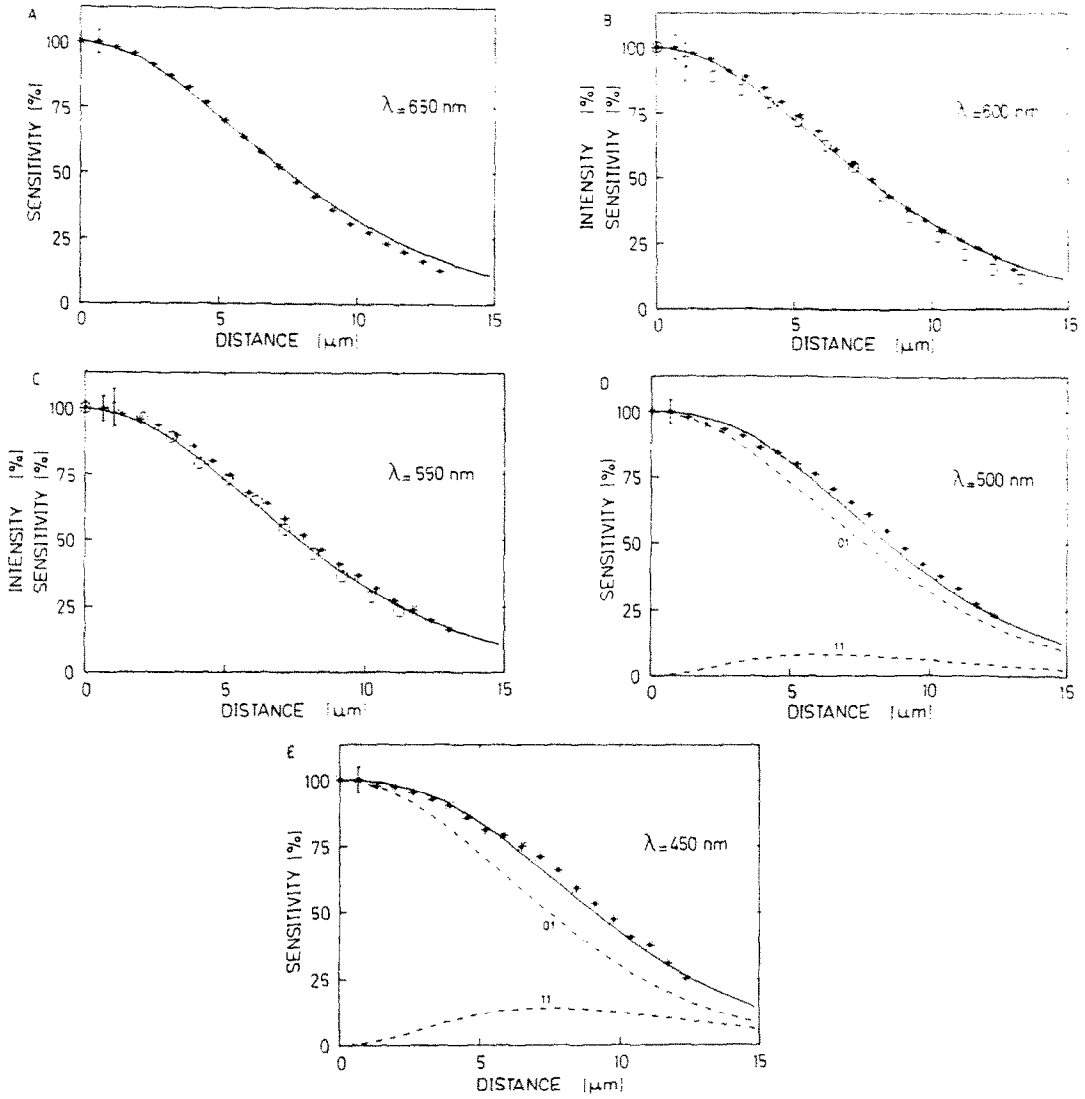

Fig. 8. Electrophysiological measurements (asterisks), radiation patterns (open circles), and theoretical fits (continuous curves) of the Stiles–Crawford effect. Focal distance: 80 μm; $\bar{n} = 0.25$; fiber diameter: 1.8 μm; wavelengths: (A) 650 nm; (B) 600 nm; (C) 550 nm; (D) 500 nm; (E) 450 nm. The lens diameter was ca. 30 μm.

that the measurements are made on a superposition of the radiation of seven waveguides, the agreement between theory and experiment in Fig. 6 is fair.

Electrophysiological measurements of the Stiles–Crawford effect in the fly's eye are shown in Fig. 7(a) (600 nm) and 7(b) (450 nm). Together with measurements at other wavelengths, the curves are shown again in Fig. 8 (asterisks), after transformation to a linear sensitivity scale. The facet belonging to the penetrated sense cell was also photographed, and the resulting radiation intensity curves are also shown in Fig. 8(b) and 8(c) (open circles). Moreover, the continuous curves in Fig. 8 are theoretical fits, with two free variables: the focal distance f (for all wavelengths) and the relative weighting of the two modes (for the shorter wavelengths). As already explained in the section on Theory, the relative weighting of the modes for the shorter wavelengths (500 and 450 nm in Fig. 8) differs from the relative weighting for the optical measurements [Fig. 6(c)]. Apart from this expected difference, the two experimental methods agree very well with each other and with the theoretical calculations.

DISCUSSION

Optical parameters obtained from the Stiles–Crawford effect

We have seen that the Stiles–Crawford effect is present in the eye of the blowfly at the level of single ommatidia. It can be measured electrophysiologically from single cell recordings, optically from the light radiating out of the rhabdomeres, and it can be calculated using a model incorporating waveguide effects in the photoreceptors. Up till now we have focused on the question of how well waveguide

theory can explain the measured Stiles–Crawford curves. But we might as well reverse the question, and ask what information we can obtain about the dioptrical system if we take the theoretical framework for granted. This appears to be justified for the fly visual system, but we will also assume that it is the main explanation for the Stiles–Crawford effect in the human eye.

In the human eye the focal distance f is well known, whilst there is some uncertainty with regard to $\tilde{n} = (n_1^2 - n_2^2)^{1/2}$. Assuming that the measured Stiles–Crawford effect (e.g. Stiles 1937) is caused mainly by the waveguide properties of the cones, we can infer $\tilde{n}$ from them. According to Stiles (1937) the curve is described by $\log \eta = -pd^2$, with $p = 0.063$ for the longest wavelengths. For these wavelengths the cones (or their inner segments) are probably guiding only the first order mode (Snyder and Pask 1973).

Assuming a focal distance of the lens of 17 mm, a wavelength of 700 nm, and $p = 0.063$, a fiber diameter of 2 μm then yields $\tilde{n} = 0.35$ according to the theoretical model used in the present paper; alternatively, a fiber diameter of 1 μm yields $\tilde{n} = 0.39$. These values are in good agreement with the measurements of Enoch and Tobey (1981), but not with the value

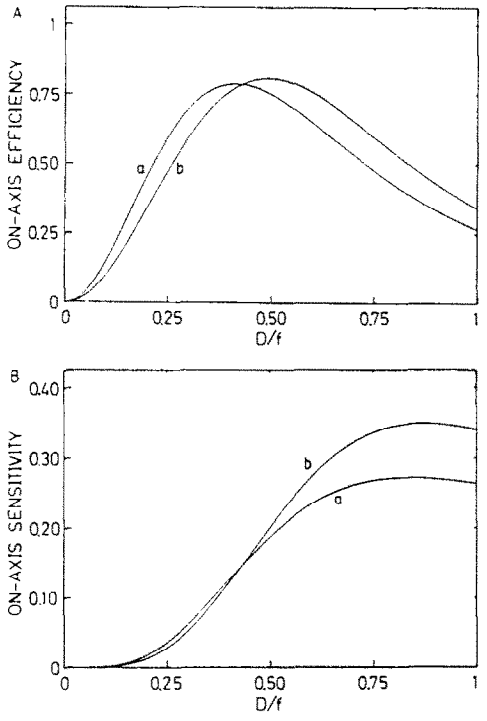

Fig. 9.(A) The on-axis efficiency for varying D/f (with D the lens diameter, and f the focal distance) for $\tilde{n} = 0.25$ (curve a) and $\tilde{n} = 0.39$ (curve b). Fiber diameter: 2 μm; wavelength: 600 nm. The on-axis efficiency is that part of the light falling on-axis on the lens that is propagated in the waveguide. (B) The on-axis efficiency times the lens surface, with the focal distance constant, and varying D. Parameters as in (A). The units are normalized to the power falling on the lens for the largest lens diameter ($D/f = 1$). Curve a: $\tilde{n} = 0.25$; curve b: $\tilde{n} = 0.39$.

$\tilde{n} = 0.19$ used by Snyder and Pask (1973) in their theoretical study on the Stiles–Crawford effect. The reason is, that in their calculations the illumination is supposed to be limited to the fiber entrance (Snyder *et al.*, 1973), whereas in the calculations of the present paper the illumination is supposed to be much wider than the fiber diameter, a situation very likely encountered in the fly's eye. Moreover, the experimental data acquired could not be satisfactorily explained when the Snyder and Pask assumption was made. But if the photoreceptors are packed very closely, as in the vertebrate fovea, the modes might be perturbed by neighbouring photoreceptors (Wijngaard, 1981), and an intermediate case could result.

Most parameters of the dioptrical apparatus of the fly are rather well known. Moreover, in the case of one mode the value of the fiber diameter is not very critical for the Stiles–Crawford effect. The two most important parameters are the focal distance f and $\tilde{n}$. The half-width of the theoretical Stiles–Crawford curves is proportional to f, and approximately proportional to $\tilde{n}$. For fly rhabdomeres $\tilde{n}$ has been measured (Beersma *et al.*, 1982; Kirschfeld and Snyder, 1976), and is about 0.25. When this value for $\tilde{n}$ is used, Stiles–Crawford measurements performed in various parts of the fly's eye indicate that the F-number of the lenses is not constant, being larger in the dorsal-frontal part ($F \simeq 3$) than ventrally and laterally ($F = 2$–2.5).

Consequences of a variable F

If the F-number of the lenses of the fly's eye is not constant over the eye, what are then the consequences of this variation for the absolute sensitivity of the visual sense cells? The question also bears importance for the vertebrate eye, because its pupil diameter is variable, that is, its F-number is variable. In Fig. 9(a) the theoretically calculated on-axis efficiency is shown as a function of $1/F = D/f$ (lens diameter divided by focal distance). The on-axis efficiency of a lens-photoreceptor system is that part of the light falling on-axis on the lens that is propagated in the photoreceptor. In Fig. 9(a) the absorption in the interocular media is neglected, and the lens is assumed to be aberration-free.

Both are good assumptions for the eye of the blowfly, but less well for the human eye. Nevertheless, including interocular absorption and lens aberrations would yield similar results. In Fig. 9(a) two curves are drawn, one with $\tilde{n} = 0.25$ (the fly's case), and one with $\tilde{n} = 0.39$ (as we inferred above for human cones or their inner segments). It appears that the F-number yielding the highest on-axis efficiency, depends on $\tilde{n}$, and that the curves are relatively broad: the efficiency can be high even if the F-number is not optimal.

A larger lens can catch more light than a smaller one, thus if we want to know the total power caught on-axis, the curves of Fig. 9(a) must be multiplied by the lens surface. The result of this operation is shown

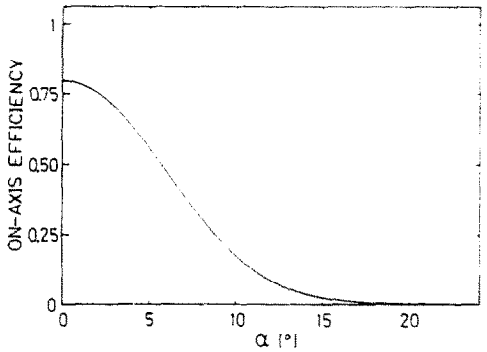

Fig. 10. The effect of deviations from alignment towards the center of the lens on the on-axis efficiency; $\bar{n} = 0.25$; fiber diameter: 2 μm; wavelength: 600 nm. The angle α is the angle between the fiber axis and the line joining the fiber tip and the center of the back principle plane of the lens.

in Fig. 9(b). We see, that it is useless to enlarge the diameter of a lens beyond a certain limit (depending on $\bar{n}$), because the extra light will not be caught by the photoreceptors. The amount of light captured will even be reduced slightly by destructive interference. Moreover, light which is not caught would deteriorate the visual acuity by leaking to neighbouring receptors and stimulating them.

Consequences of alignment

In Fig. 3 it was shown that the rhabdomeres in the eye of the blowfly are aligned towards the center of the lens. The exact position of the convergence point is somewhat uncertain, but it is close to the principle plane of the lens. Interestingly, the same phenomenon, convergence towards the center of the lens, has been found in the human eye (review: Enoch 1981).

Figure 10 suggests a possible explanation for these phenomena. The on-axis efficiency is given as a function of the angle α between the axis of the photoreceptor and the line joining the photoreceptor tip and the center of the lens (the back principle plane); thus, if $\alpha = 0$ the receptor is perfectly aligned towards the center of the lens. As we see in Fig. 10, the on-axis efficiency is highest with perfect alignment, and it depends quite critically on the angle α. Figure 10 assumes an aberration-free lens, and paraxial rays. This is again a good approximation for the fly's eye, but possibly the calculations would yield similar results when aberrations present in the vertebrate eye are taken into account. In Fig. 10 only the first order mode is present; with more modes (shorter wavelengths) the situation is more complicated, but leads to the same conclusions. Of course, Fig. 10 immediately suggests that a mechanism for achieving alignment could be based on maximizing the amount of light captured: a misalignment of only 2.5° causes a 10% reduction in sensitivity. It has to be noted, however, that an alternative explanation for the alignment of fly rhabdomeres has been proposed by Wijngaard and Stavenga (1975). They argue that optical coupling between the rhabdomeres in the same ommatidium could be minimized by the fact that, because of the alignment, the rhabdomeres diverge below their tips.

Acknowledgements—I wish to thank Drs D. G. Stavenga and R. C. Hardie for fruitful discussions and critical comments on the manuscript, and H. L. Leertouwer, E. Nienhuis and U. J. Douma for expert technical advice and assistance. This research was partially supported by the Dutch Organization for the Advancement of Pure Research (Z.W.O.) through the Foundation for Biophysics.

REFERENCES

Baylor D. A. and Fettiplace R. (1975) Light path and photon capture in turtle photoreceptors. *J. Physiol.* **248**, 433–464.

Beersma D. G. M. (1979) Spatial characteristics of the visual field of flies. Thesis, Univ. of Groningen.

Beersma D. G. M., Hoenders B. J., Huiser A. M. J. and Toorn P. van (1982) Refractive index of the fly rhabdomere. *J. opt. Soc. Am.* **72**, 583–588.

Crawford B. H. (1972) The Stiles–Crawford effects and their significance in vision. In *Handbook of Sensory Physiology* (Edited by Jameson D. and Hurvich L. M.), Vol. VII/4, pp. 470–483. Springer, Berlin.

Enoch J. M. (1963) Optical properties of retinal photoreceptors. *J. opt. Soc. Am.* **53**, 71–85.

Enoch J. M. (1981) Retinal receptor orientation and photoreceptor optics. In *Vertebrate Photoreceptor Optics* (Edited by Enoch J. M. and Tobey F. L. Jr), pp. 127–168. Springer, Berlin.

Enoch J. M. and Bedell H. E. (1981) The Stiles–Crawford effects. In *Vertebrate Photoreceptor Optics* (Edited by Enoch J. M. and Tobey F. L. Jr), pp. 83–126. Springer, Berlin.

Enoch J. M. and Tobey F. L. Jr (1981) Waveguide properties of retinal photoreceptors: Techniques and observations. In *Vertebrate Photoreceptor Optics* (Edited by Enoch J. M. and Tobey F. L. Jr), pp. 169–218. Springer, Berlin.

Franceschini N. (1975) Sampling of the visual environment by the compound eye of the fly: Fundamentals and applications. In *Photoreceptor Optics* (Edited by Snyder A. W. and Menzel R.), pp. 98–125. Springer, Berlin.

Goodman J. W. (1968) *Introduction to Fourier Optics*. McGraw-Hill, New York.

Groot P. J. de (1980) Optical properties of foveal receptors. Thesis, Univ. of Utrecht.

Hardie R. C. (1979) Electrophysiological analysis of fly retina. I: Comparative properties of R1-6 and R7 and 8. *J. comp. Physiol.* **129**, 19–33.

Hardie R. C. (1985) Functional organization of the fly retina. In *Prog. Sens. Physiol.* (Edited by Ottoson D.), Vol. 5, pp. 1–80. Springer, Berlin.

Hateren J. H. van (1984) Waveguide theory applied to optically measured angular sensitivities of fly photoreceptors. *J. comp. Physiol.* **A154**, 761–771.

Horowitz B. R. (1981) Theoretical considerations of the retinal receptor as a waveguide. In *Vertebrate Photoreceptor Optics* (Edited by Enoch J. M. and Tobey F. L. Jr), pp. 219–300. Springer, Berlin.

Horridge G. A., Mimura K. and Hardie R. C. (1976) Fly photoreceptors. III: Angular sensitivity as a function of wavelength and the limits of resolution. *Proc. R. Soc. Lond. B* **194**, 151–177.

Kirschfeld K. and Franceschini N. (1968) Optische Eigenschaften der Ommatidien im Komplexauge von Musca. *Kybernetik* **5**, 47–52.

Kirschfeld K. and Snyder A. W. (1976) Measurements of a photoreceptor's characteristic waveguide parameter. *Vision Res.* **16**, 775–778.

Marcuse D. (1974) *Theory of Dielectric Optical Waveguides*. Academic Press, New York.

Muijser H. (1979) A micro-electrode amplifier with an infinite resistance current source for intracellular measurements of membrane potential and resistance changes under current clamp. *Experientia* **35**, 912–913.
O'Brien B. (1946) A theory of the Stiles and Crawford effect. *J. opt. Soc. Am.* **36**, 506–509.
Safir A. and Hyams L. (1969) Distribution of cone orientations as an explanation of the Stiles–Crawford effect. *J. opt. Soc. Am.* **59**, 757–765.
Smakman J. G. J., Hateren J. H. van and Stavenga D. G. (1984) Angular sensitivity of blowfly photoreceptors: intracellular measurements and wave-optical predictions. *J. comp. Physiol.* **A155**, 239–247.
Smakman J. G. J. and Pijpker B. A. (1983) An analog-digital feedback system for measuring photoreceptor properties with an equal response method. *J. Neurosci. Meth.* **8**, 365–373.
Snyder A. W. (1969) Excitation and scattering of modes on a dielectric optical fiber. *IEEE Trans. Microwave Theory Tech.* **17**, 1138–1144.
Snyder A. W. (1975) Photoreceptor optics—theoretical principles. In *Photoreceptor Optics* (Edited by Snyder A. W. and Menzel R.), pp. 38–55. Springer, Berlin.
Snyder A. W. and Love J. D. (1983) *Optical Waveguide Theory*. Chapman & Hall, London.
Snyder A. W. and Pask C. (1973) The Stiles–Crawford effect—explanation and consequences. *Vision Res.* **13**, 1115–1137.
Snyder A. W., Pask C. and Mitchell D. J. (1973) Light-acceptance property of an optical fiber. *J. opt. Soc. Am.* **63**, 59–64.
Stavenga D. G. (1975) Optical qualities of the fly eye—An approach from the side of geometrical, physical and waveguide optics. In *Photoreceptor Optics* (Edited by Snyder A. W. and Menzel R.), pp. 126–144. Springer, Berlin.
Stiles W. S. (1937) The luminous efficiency of monochromatic rays entering the eye pupil at different points and a new color effect. *Proc. R. Soc. Lond. B* **123**, 90–118.
Stiles W. S. and Crawford B. H. (1933) The luminous efficiency of rays entering the eye pupil at different points. *Proc. R. Soc. Lond. B* **112**, 428–450.
Toraldo di Francia G. (1949) Retinal cones as dieletric antennas. *J. opt. Soc. Am.* **39**, 324.
Vogt K. (1983) Is the fly visual pigment a rhodopsin? *Z. Naturforsch.* **38c**, 329–333.
Wijngaard W. (1981) Theoretical considerations of optical interactions in an array of retinal receptors. In *Vertebrate Photoreceptor Optics* (Edited by Enoch J. M. and Tobey F. L. Jr), pp. 301–324. Springer, Berlin.
Wijngaard W. and Stavenga D. G. (1975) On optical crosstalk between fly rhabdomeres. *Biol. Cybernet.* **18**, 61–67.

APPENDIX

The theoretical calculations (see also Snyder, 1969; van Hateren, in preparation) are done on a simplified model, that consists of a cylindrical waveguide. This waveguide is weakly guiding, that is, the refractive indices of its interior and exterior are nearly the same (Snyder, 1969; Marcuse, 1974). The Kirchhoff approximation is used for the excitation (or radiation) of the modes. Only bound modes are considered, and it is assumed that neighbouring receptors are not optically coupled.

The angular sensitivity (or the farfield radiation pattern) of this waveguide is for a mode $\nu\mu$ given by

$$S(\phi) = |a_{\nu\mu}(\rho)|^2 \tag{2}$$

with

$$\rho = \frac{n_0 \sin \phi}{\lambda} \tag{3}$$

where ϕ is the angle between the axis of the waveguide and the direction of propagation of the incoming light, n_0 the refractive index of the medium in front of the waveguide, and λ the free space wavelength of the light; $a_{\nu\mu}(\rho)$ is given by

$$a_{\nu\mu}(\rho) = \left(\frac{2}{n_0}\right)^{1/2} \frac{\beta}{k} A \pi F(\rho) \tag{4}$$

where β is the propagation constant of the mode (see below), k is the free space wavenumber of the light ($k = 2\pi/\lambda$), A is a normalization constant (see below), and $F(\rho)$ is given by

$$F(\rho) = \left[\frac{b^2}{U^2 - (2\pi\rho b)^2} + \frac{b^2}{W^2 + (2\pi\rho b)^2}\right] \times \left[2\pi\rho b J_\nu(U) J_{\nu-1}(2\pi\rho b) - U J_{\nu-1}(U) J_\nu(2\pi\rho b)\right] \quad \text{for} \quad U \neq 2\pi\rho b \tag{5}$$

$$F(\rho) = \frac{b^2}{2}\left[J_\nu^2(U) - J_{\nu-1}(U) J_{\nu+1}(U)\right] \quad \text{for} \quad U = 2\pi\rho b \tag{6}$$

where b is the radius of the waveguide, and J_ν is a Bessel function of the first kind. In the calculations of Snyder and Pask (1973) the term with W^2 in equation (5) is not present. U and W are solutions of the characteristic equation of the fiber

$$U \frac{J_{\nu+1}(U)}{J_\nu(U)} = W \frac{K_{\nu+1}(W)}{K_\nu(W)} \tag{7}$$

with

$$U^2 + W^2 = \left(\frac{2\pi b}{\lambda}\right)^2 (n_1^2 - n_2^2) = V^2 \tag{8}$$

where K_ν is a modified Hankel function of the first kind, n_1 the refractive index of the waveguide, n_2 that of the medium surrounding it, and V a parameter that determines the number of propagated modes and their shape. Now the propagation constant is given by

$$\beta = (n_1^2 k^2 - U^2/b^2)^{1/2} \tag{9}$$

and the normalization constant A by

$$A = \left[-\tfrac{1}{4} e_\nu \pi \frac{\beta}{k} b^2 J_{\nu-1}(U) J_{\nu+1}(U)(1 + U^2/W^2)\right]^{-1/2} \tag{10}$$

where $e_\nu = 2$ for $\nu = 0$ and $e_\nu = 1$ for $\nu \neq 0$.

The on-axis sensitivity (Fig. 9) of the entire lens-fiber system is given by

$$S = \left|2\frac{\beta}{k} A \left(\frac{2}{\pi n_0}\right)^{1/2} \frac{2\lambda f}{D} \pi^2 \int_0^{D/2f} \mathrm{d}\rho\, \rho F(\rho)\right|^2 \tag{11}$$

Figure 10 was calculated by straightforward integrating the product of the fields of an Airy diffraction pattern and of the first order mode, incorporating phase variations caused by the skewness of the fiber.